

References and Notes

1. S. Poethig, in *Contemporary Problems in Plant Anatomy*, R. A. White and W. C. Dickson, Eds. (Academic Press, New York, 1984), pp. 235–259.
2. L. G. Smith, B. Greene, B. Veit, S. Hake, *Development* **116**, 21 (1992); D. Jackson, B. Veit, S. Hake, *ibid.* **120**, 404 (1994); M. Scanlon, R. G. Schneeberger, M. Freeling, *ibid.* **122**, 1683 (1996).
3. R. G. Schneeberger, P. W. Beecraft, S. Hake, M. Freeling, *Genes Dev.* **9**, 2292 (1995).
4. D. Haraven, T. Gutfinger, A. Parnis, Y. Eshed, E. Lifschitz, *Cell* **84**, 735 (1996); N. R. Sinha, R. E. Williams, S. Hake, *Genes Dev.* **7**, 787 (1993); C. Lincoln, J. Long, J. Yamaguchi, K. Serikawa, S. Hake, *Plant Cell* **6**, 1859 (1994); K. J. Muller *et al.*, *Nature* **374**, 727 (1995); G. Chuck, C. Lincoln, S. Hake,

- Plant Cell* **8**, 1277 (1996); R. E. Williams-Carrier, Y. S. Lie, S. Hake, P. G. Lemaux, *Development* **124**, 3737 (1997).
5. R. A. Kerstetter, D. Laudencia-Chinguanco, L. G. Smith, S. Hake, *Development* **124**, 3045 (1997).
6. R. Schneeberger, M. Tsiantis, M. Freeling, J. A. Langdale, *ibid.* **125**, 2857 (1998).
7. Supplementary material is available at www.sciencemag.org/feature/data/986218.shl
8. R. Waites, H. R. N. Selvadurai, I. R. Oliver, A. Hudson, *Cell* **93**, 779 (1998).
9. M. Tsiantis and J. A. Langdale, unpublished results.
10. R. Waites and A. Hudson, unpublished results.
11. ———, *Development* **121**, 2143 (1995).
12. M. Freeling, *Dev. Biol.* **153**, 44 (1992).
13. A. W. Eichler, *Zur Entwicklungsgeschichte des Blattes*

- mit Besonderer Berücksichtigung der Nebenblatt-Bildung* (Marsburg, 1861).
14. D. R. Kaplan, *Quart. Rev. Biol.* **48**, 437 (1973).
15. G. J. Muehlbauer, J. E. Fowler, M. Freeling, *Development* **124**, 5097 (1997).
16. We thank A. Hudson and his group (Edinburgh) for help with in situ hybridizations, T. Brunnell for *Mu* primers, G. Akgun for technical assistance, R. Tyers and L. Jesaitis for discussions of leaf-zone, and J. Baker for photography. Work in J.A.L.'s lab is funded by the UK Biotechnology and Biological Sciences Research Council and the Gatsby Charitable Foundation. Work in M.F.'s lab was funded by NIH fellowship GM114578 to R.S. and NIH grant GM42610 to M.F. M.T. is the recipient of a University of Oxford Glasstone Fellowship.

3 November 1998; accepted 3 March 1999

Apaf-1 and Caspase-9 in p53-Dependent Apoptosis and Tumor Inhibition

M. S. Soengas,¹ R. M. Alarcón,² H. Yoshida,^{3*} A. J. Giaccia,² R. Hakem,³ T. W. Mak,³ S. W. Lowe^{1†}

The ability of p53 to promote apoptosis in response to mitogenic oncogenes appears to be critical for its tumor suppressor function. Caspase-9 and its cofactor Apaf-1 were found to be essential downstream components of p53 in Myc-induced apoptosis. Like p53 null cells, mouse embryo fibroblast cells deficient in Apaf-1 and caspase-9, and expressing *c-Myc*, were resistant to apoptotic stimuli that mimic conditions in developing tumors. Inactivation of Apaf-1 or caspase-9 substituted for p53 loss in promoting the oncogenic transformation of *Myc*-expressing cells. These results imply a role for Apaf-1 and caspase-9 in controlling tumor development.

The p53 tumor suppressor promotes cell cycle arrest or apoptosis in response to several cellular stresses, including mitogenic oncogenes (1). For example, the *c-Myc* oncogene induces uncontrolled proliferation but also activates p53 to promote apoptosis (2). Although the balance between Myc-induced proliferation and cell death is determined by genotype and external signals, Myc-induced apoptosis inhibits oncogenic transformation (3). Consistent with this view, *Myc* and other mitogenic oncogenes activate p53 through p19^{ARF}, a tumor suppressor encoded at the INK4a/ARF locus (4). The ARF-p53 pathway is disabled in most human cancers, which implies that an oncogene-activated p53-dependent apoptosis pathway contributes to tumor suppression (4).

How activated p53 promotes apoptosis is unclear, but it may involve Bax (5, 6), a series of p53-inducible genes known as PIGs (7), or signaling through Fas-related pathways (8). Other p53 effectors might include caspases, a family of cysteine proteases that execute apoptotic cell death (9). Signaling

procaspases associate with specific adaptor molecules that facilitate caspase activation by induced proximity (10). For example, caspase-9 (Casp9) associates with Apaf-1, and oligomerization of this complex in the presence of cytochrome c can activate a caspase cascade (11). Studies with knockout mice show that the requirement for different death effectors during apoptosis is highly cell-type- and stimulus-specific (12–15). Because p53-dependent apoptosis limits tumor development, the caspase-adaptor complex (or complexes) that acts downstream of p53 may participate in tumor suppression. However, the observation that caspase inhibitors do not prevent cell death induced by Myc or the p53-effector Bax suggests that caspases act too late in these death programs to have a substantial effect on long-term survival (16).

To determine the requirement for the Casp9 and Apaf-1 in apoptosis induced by Myc and p53, early-passage mouse embryo fibroblasts (MEFs) derived from Apaf-1- and Casp9-deficient mice were examined for their response to Myc. *c-Myc* or a control vector was transduced into wild-type, p53^{-/-}, Casp9^{-/-}, or Apaf-1^{-/-} MEFs with the use

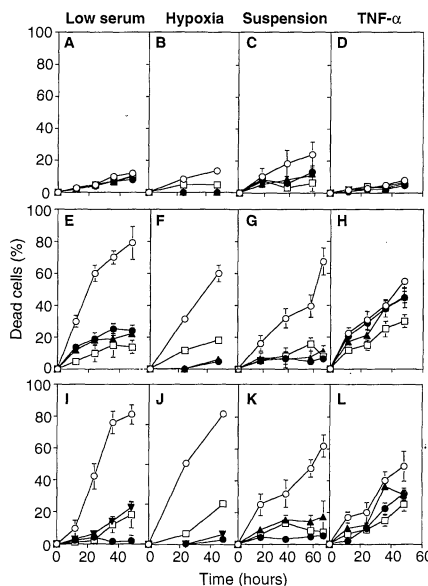


Fig. 1. Requirement for Apaf-1 and Casp9 in Myc-induced apoptosis. A control vector (A to D), *c-Myc* (E to H), or *c-Myc* and *H-rasV12* (I to L) were transduced into early passage MEFs derived from wild-type (open circles), p53^{-/-} (open squares), Casp9^{-/-} (closed circles), and Apaf-1^{-/-} (closed triangles) mice with high-titer recombinant retroviruses (17). Cell populations were incubated in growth factor-poor (low serum) medium (A, E, and I), hypoxic conditions (B, F, and J), suspension (C, G, and K), or murine TNF-α (D, H, and L) for the indicated times, and cell viability was determined by trypan blue exclusion (17, 18). Each point represents the mean ± SD of at least three experiments with two separately transduced populations. Data are normalized to the rate of spontaneous cell death occurring in untreated cells (<10% in all cases, except 25% for Myc-Ras wild-type MEFs).

¹Cold Spring Harbor Laboratory, Cold Spring Harbor, NY 11724, USA. ²Stanford University School of Medicine, Department of Radiation Oncology, Stanford, CA 94305, USA. ³Amgen Institute and Ontario Cancer Institute, Department of Medical Biophysics and Immunology, University of Toronto, Toronto, Ontario M5G 2C1, Canada.

*Present address: Department of Immunology, Medical Institute of Bioregulation, Kyushu University, Fukoka, Japan.

†To whom correspondence should be addressed. E-mail: lowe@cshl.org

REPORTS

of high-titer retroviruses (17), allowing whole populations of genotypically altered cells to be analyzed with minimal expansion in culture. The resulting populations were exposed to apoptotic stimuli that recapitulate tumor microenvironmental stresses (Fig. 1) (18). As expected, Myc sensitized wild-type cells to apoptosis after growth factor depletion (low serum) or hypoxia (19) as well as in suspension (Fig. 1). However, p53^{-/-}, Casp9^{-/-}, and Apaf-1^{-/-} cells expressing Myc were resistant to apoptosis under these conditions. Consistent with previous reports (20), oncogenic Ras (H-rasV12), which cooperates with Myc to transform primary cells to a tumorigenic state, did not prevent Myc-induced apoptosis but slightly enhanced spontaneous cell death (Fig. 1). As in cells expressing Myc alone, disruption of p53, Apaf-1, or Casp9 in cells coexpressing Myc and Ras (Myc-Ras MEFs) prevented apoptosis after serum depletion or hypoxia or in suspension (Fig. 1, I to K). In contrast, neither Apaf-1 nor Casp9 was required for tumor necrosis factor (TNF)-induced apoptosis, a program in which p53 is largely dispensable (Fig. 1, H and L) (21). Moreover, p53-dependent apoptosis in Myc-expressing cells did not require the caspase-8–FADD pathway or caspase-2 (22, 23). Of note, the caspase inhibitor zVAD.fmk was three times less efficient at blocking apoptosis of the p53-dependent deaths than genetic deletion of Apaf-1 or Casp9 (24), which implies that zVAD.fmk is an ineffective inhibitor of Casp9.

The similar requirement for p53, Apaf-1, and Casp9 in Myc-induced apoptosis suggests that these genes act in the same pathway. Apaf-1 and Casp9 do not act upstream of p53, because c-Myc or the combination of c-Myc plus Ras efficiently induced p53 protein and

activity in Apaf^{-/-} and Casp9^{-/-} MEFs (Fig. 2A). To determine whether Apaf-1 and Casp9 act downstream of p53, a temperature-sensitive p53 (p53val138) fused to green fluorescent protein (GFP) was introduced into wild-type, p53^{-/-}, Apaf-1^{-/-}, and Casp9^{-/-} Myc-Ras MEFs (17), and the apoptotic response of GFP-positive cells was determined at the restrictive (39°C) or permissive (33°C) temperature (Fig. 2B). At 33°C, p53 induced massive apoptosis in wild-type cells and rescued the apoptotic defect in p53^{-/-} cells, but it had no pro-apoptotic effect in Apaf-1^{-/-} or Casp9^{-/-} cells.

p53 activation by oncogenes and tumor microenvironmental stresses may provide a natural brake to tumor development (1, 4). If Apaf-1 and Casp9 are required for p53 action under these circumstances, then inactivation of either one should facilitate oncogenic transformation. To test this hypothesis, we assayed wild-type, p53^{-/-}, Apaf-1^{-/-}, and Casp9^{-/-} Myc-Ras MEFs for their ability to produce colonies in soft agar (Fig. 3) and form tumors in immunocompromised mice. Consistent with the ability of p53 to suppress transformation, p53-deficient cells formed >100 times the number of colonies in soft agar as wild-type cells (Fig. 3A). Cells without Apaf-1 or Casp9 formed a similar amount of colonies as p53-deficient cells. Thus, inactivation of Apaf-1 or Casp9 can enhance the long-term survival of oncogenically transformed cells.

To determine the potential impact of Apaf-1 and Casp9 inactivation on tumor development, we injected wild-type, p53^{-/-}, Apaf-1^{-/-}, and Casp9^{-/-} Myc-Ras MEFs subcutaneously into immunocompromised mice and monitored for tumors at the sites of injection. As expected, p53 reduced the tumorigenicity of Myc-Ras-

transformed cells (Table 1 and Fig. 4). Hence, at low numbers of injected cells, wild-type cells produced tumors at a lower frequency than p53^{-/-} cells, and the tumors that formed grew at dramatically reduced rates (Table 1 and Fig. 4). At higher cell numbers, wild-type cells produced tumors more readily (Table 1), perhaps because higher concentrations of autocrine survival factors protected cells from apoptosis in vivo. Still, tumors derived from p53-deficient cells displayed more rapid growth.

Apaf-1 and Casp9 had a profound effect on suppressing the tumorigenicity of Myc-Ras MEFs (Table 1 and Fig. 4). Inactivation of Apaf-1 and Casp9 substantially reduced the number of cells required to form tumors (Table 1), which grew at rates similar to tumors derived from p53-deficient cells (Fig. 4). This enhanced tumorigenicity was most likely due to inefficient apoptosis, because Apaf-1^{-/-} and Casp9^{-/-} Myc-Ras MEFs displayed marked apoptotic defects (see Fig. 1) and showed no differences in proliferation (Fig. 4). Moreover, tumors derived from wild-type cells displayed two- to fourfold more apoptotic bodies than tumors derived from Apaf-1^{-/-} or Casp9^{-/-} cells (24). Importantly, all injected Myc-Ras cells were nonclonal populations that were min-

Fig. 2. Apaf-1 and Casp9 act downstream of p53 to promote apoptosis. (A) Immunoblot analysis of the indicated proteins in vector control (lanes V) or in two independent populations (lanes 1 and 2) of Myc-Ras-transformed MEFs of the indicated genotypes. For wild-type cells, populations 1 and 2 correspond to MEFs extracted from littermates of Apaf-1^{-/-} and Casp9^{-/-} mice, respectively. Thirty micrograms of lysate was prepared from exponentially growing cells and separated onto 8% SDS-polyacrylamide gels for detection of c-Myc (N-262, Santa Cruz), p53 (CM-5, Novocastra), and Mdm2 (mAb 2A10, provided by A. Levine, Rockefeller University) or onto 12% gels for detection of Ras (OP23, Calbiochem) by standard immunoblot procedures. Expression of α -tubulin (clone B-5-1-2, Sigma) is shown as a loading control. (B) Viability of Myc-Ras-transformed cells expressing a temperature-sensitive p53 at the restrictive (39°C, white bars) or permissive (33°C, hatched bars) temperature for wild-type p53 expression. Myc-Ras MEFs were transduced with a retrovirus expressing human p53val138 fused to GFP. Infected cell populations (>80% GFP-positive) were placed in medium containing 1% FBS and retained at 39°C or transferred to 33°C for 48 hours. Cell viability was determined by trypan blue exclusion and by DAPI staining (12). (C) Representative fluorescence micrographs of cells grown at 33°C showing GFP or DAPI (1 μ g/ml) fluorescence to monitor p53 expression or chromatin condensation, respectively.

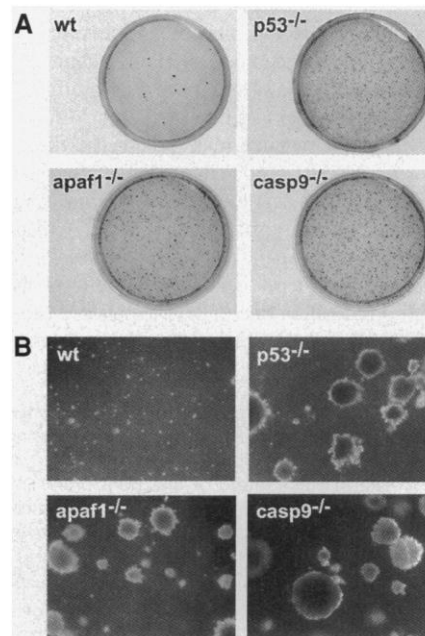
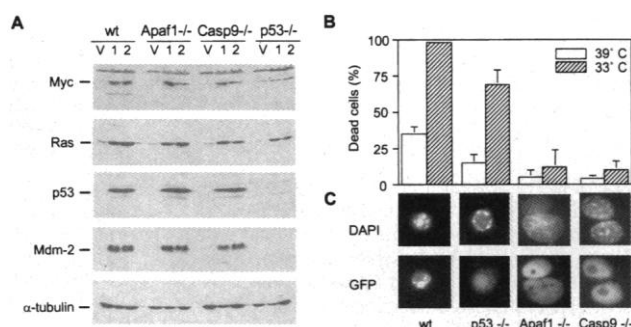


Fig. 3. Effect of Apaf-1 and Casp9 on colony formation in soft agar; 2×10^4 cells of the indicated genotypes were resuspended in 0.3% Noble agar (in DMEM supplemented with 10% FBS) and plated on 6-cm plates containing a solidified bottom layer (0.5% Noble agar in growth medium). Giemsa staining (A) and phase-contrast microscopy (B) of a representative experiment 2 weeks after plating. The plating efficiencies determined by counting colonies containing ≥ 40 cells in random fields were <1%, 65%, 75%, and 80% for wild-type (wt), Apaf-1^{-/-}, Casp9^{-/-}, and p53^{-/-} MEFs, respectively.

imally passaged in culture, yet Apaf-1^{-/-} and Casp9^{-/-} Myc-Ras MEFs formed tumors rapidly (tumors were visible 4 days after injection). Therefore, it is unlikely that rare secondary mutations contribute to tumor acceleration. These results demonstrate that defects in the effector mechanism of p53-dependent apoptosis can facilitate tumor development.

Cytochrome c is required for activation of pro-Casp9, and cytochrome c release from mitochondria appears to be essential for some apoptotic programs (25). Of note, both pro-apoptotic oncogenes and p53 can affect mitochondrial function. For example, the adenovirus *E1A* oncogene [which also activates p53 (26)] and the p53 effector Bax facilitate cytochrome c release (27). Furthermore, the *PIGs* may act to influence redox metabolism and the mitochondrial permeability transition (7). Although it is possible that p53-mediated activation of the Fas pathway might indirectly target the mitochondria through caspase-8 (8, 28), we see no evidence that Apaf-1 and Casp9 are required for Fas or TNF-induced apoptosis (13) (Fig. 1). Therefore, our data support the view that immediate effectors of p53 in apoptosis target the mitochondria, thereby releasing cytochrome c to activate Casp9.

It has been unclear whether inactivation of apoptotic components acting downstream of cytochrome c should enhance long-term survival or only delay cell death (25). We show that disruption of Apaf-1 or Casp9 allows efficient colony formation in soft agar and rapid tumor development in nude mice. These data imply that Apaf-1 or Casp9 actively limits tumor development and suggest that cytochrome c release is not necessarily a lethal event. Perhaps the ability of Apaf-1 or Casp9 deficiency to promote long-term cell survival reflects the high proliferation rate of *Myc*-expressing cells, which may allow substantial cell accumulation

as a result of inefficient cell death. Alternatively, the ability of cytochrome c release to commit a cell to death may depend on cell type, genetic background, or apoptotic stimulus.

Essential components of p53 apoptotic pathways act as tumor suppressors. For example, p19^{ARF} and Bax act upstream or downstream of p53 in oncogene-induced apoptosis, respectively, and mutations in either gene facilitate tumorigenesis in mice and humans (4, 6). Although mutations in Apaf-1 or Casp9 genes have not been described, each maps to loci disrupted in human tumors. Apaf-1 is located on chromosome 12q22-12q23 (15), a region that is altered in some pancreatic and ovarian carcinomas (29). Casp9 is located at chromosome 1p34-1p36.1 (30), a hotspot for loss of heterozygosity in several cancers, including some neuroblastomas (31). Interestingly, many neuroblastomas tolerate *N-Myc* amplification but rarely harbor p53 mutations (31-32), and neuronal hyperplasia is one of the hallmarks of Casp9-deficient mice (18). Irrespective of the frequency at which Apaf-1 and Casp9 are mutated in human cancers, our data clearly

demonstrate that disruption of the effector mechanisms of apoptosis can facilitate oncogenic transformation and tumor development.

References and Notes

1. A. J. Giaccia and M. B. Kastan, *Genes Dev.* **12**, 2973 (1998); C. Prives, *Cell* **95**, 5 (1998).
2. H. Hermeking and D. Eick, *Science* **265**, 2091 (1994); A. J. Wagner, J. M. Kokontis, N. Hay, *Genes Dev.* **8**, 2817 (1994).
3. G. Evan and T. Littlewood, *Science* **281**, 1317 (1998).
4. T. Kamijo et al., *Cell* **91**, 649 (1997); E. de Stanchina et al., *Genes Dev.* **12**, 2434 (1998); F. Zindy et al., *ibid.*, p. 2424; S. Bates et al., *Nature* **395**, 124 (1998); I. Palmero, C. Pantoja, M. Serrano *ibid.*, p. 125; J. Pomerantz et al., *Cell* **92**, 713 (1998); A. Radfar et al., *Proc. Natl. Acad. Sci. U.S.A.* **95**, 13194 (1998); C. J. Sherr, *Genes Dev.* **12**, 2984 (1998).
5. T. Miyashita and J. C. Reed, *Cell* **80**, 293 (1995).
6. M. E. McCurrach et al., *Proc. Natl. Acad. Sci. U.S.A.* **94**, 2345 (1997); C. Yin et al., *Nature* **385**, 637 (1997).
7. K. Polyak et al., *Nature* **389**, 300 (1997).
8. L. B. Owen-Schaub et al., *Mol. Cell Biol.* **15**, 3032 (1995); M. Müller et al., *J. Exp. Med.* **188**, 2033 (1998); M. Bennett et al., *Science* **282**, 290 (1998).
9. N. A. Thornberry and Y. Lazebnik, *Science* **281**, 1312 (1998); V. Cryns and J. Yuan, *Genes Dev.* **12**, 1551 (1998).
10. X. Yang, H. Y. Chang, D. Baltimore, *Science* **281**, 1355 (1998); M. Muzio et al., *J. Biol. Chem.* **273**, 2926 (1998); Y. Hu et al., *ibid.*, p. 33489.
11. H. Zou et al., *Cell* **90**, 405 (1997); P. Li et al., *ibid.* **91**, 479 (1997); S. M. Srinivasula et al., *Mol. Cell* **1**, 949 (1998).
12. M. Woo et al., *Genes Dev.* **12**, 806 (1998).
13. R. Hakem et al., *Cell* **94**, 339 (1998); K. Kuida et al., *ibid.*, p. 325.
14. H. Yoshida et al., *ibid.*, p. 739.
15. F. Ceconi et al., *ibid.*, p. 727.
16. N. J. McCarthy et al., *J. Cell Biol.* **136**, 215 (1997); J. Xiang, D. T. Chao, S. J. Korsmeyer, *Proc. Natl. Acad. Sci. U.S.A.* **93**, 14559 (1996).
17. Primary MEFs derived from wild-type, Apaf-1^{-/-}, Casp9^{-/-}, and p53^{-/-} mice were prepared as described [M. Serrano et al., *Cell* **88**, 593 (1997) and (13)]. Stable expression of *c-Myc*, *H-RasV12*, and a COOH-terminal GFP fusion of a temperature-sensitive human p53 (Val¹³⁸) was achieved by retroviral-mediated gene transfer as described [M. Serrano et al., *Cell* **88**, 593 (1997)], except that MEFs were infected four times at 4-hour intervals. Retroviral vectors were as follows: *c-Myc/MarXII-hygro* [X. Wang et al., *Genes Dev.* **12**, 1764 (1998)]; *pBabeRas* [M. Serrano et al., *Cell* **88**, 593 (1997)]; and *pWZL-GFP p53 V138* [gift of J. Hudson].
18. For cell viability experiments, 2 × 10⁵ cells were plated in Dulbecco's modified Eagle's medium (DMEM) supplemented with 10% fetal bovine serum (FBS); 12 hours after plating, cells were placed in 0.1% FBS (growth-survival factor withdrawal), 0.2% oxygen (hypoxia), 50 μg of murine TNF-α (mTNF-α) per milliliter (Fig. 1) or in 1% FBS at the restrictive or permissive temperature for p53 expression (Fig. 2). For suspension assays, 2 × 10⁴ cells per 6-cm plate were resuspended in DMEM containing 10% FBS and added on top of solidified 0.5% Noble agar. At various times after each stimulus, floating and adherent cells were pooled and analyzed for cell viability by trypan blue exclusion and for apoptosis by 4',6-diamidino-2-phenylindole (DAPI) staining for condensed chromatin (12).
19. G. I. Evan et al., *Cell* **69**, 119 (1992); T. G. Graeber et al., *Nature* **379**, 88 (1996).
20. A. Kauffmann-Zeh et al., *Nature* **385**, 544 (1997).
21. J. S. Lanni, S. W. Lowe, E. J. Licitra, J. O. Liu, T. Jacks, *Proc. Natl. Acad. Sci. U.S.A.* **94**, 9679 (1997).
22. W.-C. Yeh et al., *Science* **279**, 1954 (1998).
23. M.S.S., J. Yuan, and S.W.L., unpublished results.
24. Data not shown.
25. G. Kroemer, B. Dallaporta, M. Resche-Rigon, *Annu. Rev. Physiol.* **60**, 619 (1998); D. R. Green and J. C. Reed, *Science* **281**, 1309 (1998).

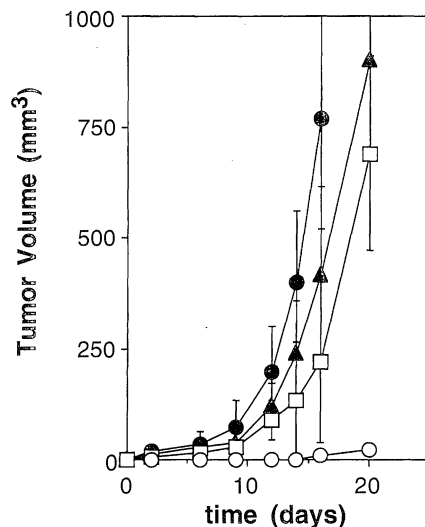


Fig. 4. Effect of Apaf-1 and Casp9 on tumorigenicity of *Myc-Ras*-transformed cells. *Myc* plus *Ras* transformed populations derived from wild type (white circles), p53^{-/-} (white squares), Apaf-1^{-/-} (black triangles), and Casp9^{-/-} (black circles) were injected subcutaneously into each rear flank of female NSW athymic nude mice (Tatonic Farms) within two passages of gene transfer. Tumor volume (V) was estimated from caliper measurements of the length (L) and width (W) as $V = (L \times W^2)/2$. For each genotype, eight sites were injected; each data point represents the mean ± SD of measurements derived from only those sites that formed tumors (see Table 1). Bromodeoxyuridine (BrdU) incorporation-DNA content analysis indicated that the cell-cycle distribution of the injected populations was similar; for example, the amounts of cells in S phase after a 4-hour BrdU pulse were 41%, 46%, 45%, and 49% for wild-type, Apaf-1^{-/-}, Casp9^{-/-}, and p53^{-/-} *Myc-Ras* cells, respectively.

Table 1. Tumorigenicity of *Myc-Ras* transformed cells. Indicated numbers of *Myc-Ras*-expressing MEFs were injected into athymic nude mice as described in Fig. 4. Ratio of injections producing tumors and volume (mean ± SD) of those tumors that formed at 2 weeks after injection are shown. ND, not determined; NA, not applicable.

Genotype	No. of injected cells	Tumors/sites injected	Tumor volume (mm ³)
Wild type	2 × 10 ⁵	0/4	NA
	5 × 10 ⁵	2/8	<10
	10 × 10 ⁵	4/4	40 ± 16
Apaf-1 ^{-/-}	2 × 10 ⁵	2/4	51 ± 21
	5 × 10 ⁵	8/8	250 ± 100
	10 × 10 ⁵	3/4	180 ± 50
Casp9 ^{-/-}	2 × 10 ⁵	4/4	70 ± 30
	5 × 10 ⁵	8/8	400 ± 200
	10 × 10 ⁵	4/4	330 ± 250
p53 ^{-/-}	2 × 10 ⁵	ND	NA
	5 × 10 ⁵	7/8	200 ± 100
	10 × 10 ⁵	ND	NA

26. S. W. Lowe and H. E. Ruley, *Genes Dev.* **7**, 535 (1993).
 27. H. O. Fearnhead *et al.*, *Proc. Natl. Acad. Sci. U.S.A.* **95**, 13664 (1998); J. M. Jurgensmeier *et al.*, *ibid.*, p. 4997; A. Gross *et al.*, *EMBO J.* **17**, 3878 (1998).
 28. X. Luo *et al.*, *Cell* **94**, 481 (1998); H. Li, H. Zhu, C. J. Xu, J. Yuan, *ibid.*, p. 491.
 29. Y. Hatta *et al.*, *Br. J. Cancer* **75**, 1256 (1997); M. Kimura *et al.*, *Cancer Res.* **58**, 2456 (1998).
 30. P. Deloukas *et al.*, *Science* **282**, 744 (1998); G. D. Schuler *et al.*, *ibid.* **274**, 540 (1996).
 31. N. C. Cheng *et al.*, *Oncogene* **10**, 291 (1995); H. Caron *et al.*, *Hum. Mol. Genet.* **4**, 535 (1995).
 32. H. Komuro *et al.*, *Cancer Res.* **53**, 5284 (1993).
 33. Supported by a Human Frontiers in Science Fellowship (M.S.S.), a Kimmel Scholar Award (S.W.L.), and grants CA64489 (A.J.G.) and CA13106 (S.W.L.) from the National Institutes of Health. All animal pro-

ocols were approved by the Cold Spring Harbor Laboratory Animal Care and Use Committee. We thank G. Hannon for retroviral vectors; J. A. Esteban, R. Malinow, G. Hannon, Y. Lazebnik, M. McCurrach, C. Schmitt, and A. Lin for help and advice; and B. Stillman and M. Spector for editorial comments.

4 January 1999; accepted 5 March 1999

Phenotypic Change Caused by Transcriptional Bypass of Uracil in Nondividing Cells

Anand Viswanathan,^{1,2} Ho Jin You,² Paul W. Doetsch^{2*}

Cytosine deamination to uracil occurs frequently in cellular DNA. In vitro, RNA polymerase efficiently inserts adenine opposite to uracil, resulting in G to A base substitutions. In vivo, uracil could potentially alter transcriptional fidelity, resulting in production of mutant proteins. This study demonstrates that in nondividing *Escherichia coli* cells, a DNA template base replaced with uracil in a stop codon in the firefly luciferase gene results in conversion of inactive to active luciferase. The level of transcriptional base substitution is dependent on the capacity to repair uracil. These results provide evidence for a DNA damage-dependent, transcription-driven pathway for generating mutant proteins in nondividing cells.

Numerous studies have shown that different types of DNA damage exert deleterious effects on replication by either blocking DNA polymerase or allowing for mutagenic bypass (1). Cells that are unable to repair certain types of DNA damage have increased mutation rates (2, 3). In contrast, much less is known concerning the interaction of DNA damage and RNA polymerases during transcription, with most studies focusing on le-

sions that permanently arrest RNA polymerase during elongation. An arrested RNA polymerase complex at a site of DNA damage serves as a signal for recruitment of the DNA excision repair machinery (4). Transcription-coupled repair allows for template strand-specific repair of a number of RNA polymerase-arresting lesions such as cyclobutane pyrimidine dimers and thymine glycol (5). However, a number of different

DNA base modifications including uracil do not arrest RNA polymerase in vitro and miscode at the lesion site, producing mutant transcripts with high efficiency (6–11). An unexplored possibility is that if similar events occur in vivo, the resulting mutant transcripts will generate mutant proteins that could alter the cellular phenotype (6, 12–14).

Uracil is a frequently occurring DNA base damage that results from the spontaneous or chemically induced deamination of cytosine and is mutagenic at the level of replication (3, 15). To determine the effect of uracil on transcription and translation in *Escherichia coli*, we used a reporter assay to measure the levels of active firefly luciferase generated from expression constructs derived from the plasmid pBest-luc containing modifications in the luciferase lysine codon 445 (Fig. 1). A unique 45-base pair (bp) Pac I–Cla I restriction fragment flanking Lys⁴⁴⁵ was removed from this construct and replaced with one of three fragments that contained in the template strand

¹Graduate Program in Genetics and Molecular Biology and ²Departments of Biochemistry and Radiation Oncology, Emory University School of Medicine, Atlanta, GA 30322, USA.

*To whom correspondence should be addressed. E-mail: medpwd@emory.edu

Fig. 1. Strategy for determining transcriptional base substitution in cells: luciferase gene modification. The pBest-luc luciferase reporter construct contains the firefly luciferase gene driven by the *E. coli* *tac* promoter and also contains the ampicillin (Amp) resistance gene (15). The 45-bp Cla I–Pac I fragment of pBest-luc was modified on the template strand at the first base of codon 445 to specify either lysine (3'-TTT-5'; Luc-WT), a stop codon (3'-ATT-5'; Luc-STOP), or lysine through transcriptional base substitution at uracil (3'-UTT-5'; Luc-U), resulting in production of wild-type, truncated, or transcriptional base substitution-mediated wild-type luciferase proteins, respectively. If DNA repair occurs through the *ung*-mediated BER pathway, codon 445 in the Luc-U construct would be converted to a stop codon (3'-ATT-5'), resulting in a truncated, inactive luciferase protein. The constructs were electroporated into *ung*⁺ or *ung*⁻ (or in some cases *mutS*⁺ or *mutS*⁻) *E. coli* strains and subsequently incubated in novobiocin-containing LB media for 30 to 240 min. Portions of cells were also plated onto LB-Amp media to determine transformation efficiency. Luciferase activity and DNA and RNA synthesis were determined from 30 to 240 min after IPTG induction. Normalized luciferase activity was determined on the basis of transformation efficiency and total luciferase activity (32). K445, Lys⁴⁴⁵.

